Brain Topography (2019) 32:859–872
https://doi.org/10.1007/s10548-019-00714-y

ORIGINAL PAPER

Accuracy of Estimating the Area of Cortical Muscle Representations from TMS Mapping Data Using Voronoi Diagrams

Andrey Yu. Chernyavskiy[1,2] · Dmitry O. Sinitsyn[1] · Alexandra G. Poydasheva[1] · Ilya S. Bakulin[1] · Natalia A. Suponeva[1] · Michael A. Piradov[1]

Received: 16 August 2018 / Accepted: 2 May 2019 / Published online: 9 May 2019

Abstract
Motor evoked potentials (MEPs) caused by transcranial magnetic stimulation (TMS) provide a possibility of noninvasively mapping cortical muscle representations for clinical and research purposes. The interpretation of such results is complicated by the high variability in MEPs and the lack of a standard optimal mapping protocol. Comparing protocols requires the determination of the accuracy of estimated representation parameters (such as the area), which is problematic without ground truth data. We addressed this problem and obtained two main results: (1) the development of a bootstrapping-based approach for estimating the within-session variability and bias of representation parameters and (2) estimations of the area and amplitude-weighted area accuracies for motor representations using this approach. The method consists in the simulation of TMS mapping results by subsampling MEPs from a single map with a large number of stimuli. We studied the extensor digitorum communis (EDC) and flexor digitorum superficialis (FDS) muscle maps of 15 healthy subjects processed using Voronoi diagrams. We calculated the (decreasing) dependency of the errors in the area and weighted area on the number of stimuli. This result can be used to choose a number of stimuli sufficient for studying the effects of a given size (e.g., the protocol with 150 stimuli leads to relative errors of 7% for the area and 11% for the weighted area in 90% of the maps). The approach is applicable to other parameters (e.g., the center of gravity) and other map processing methods, such as spline interpolation.

Keywords TMS · Motor evoked potential · Cortical muscle representation mapping · Statistical bootstrapping · Voronoi diagram · Motor cortex mapping

Introduction

Transcranial magnetic stimulation (TMS) is an effective method of noninvasively activating neuronal circuits in the brain (Di Lazzaro and Ziemann 2013). When single TMS pulses are applied to the motor cortex, motor evoked potentials (MEPs) are recorded from muscles as a result of the activation of corticospinal projections (Rotenberg et al. 2014). Systematic administration of multiple stimuli covering a region of the cortex can be used to map the cortical motor representation of a muscle, i.e., to determine the location and size of the brain area producing MEPs under stimulation (Rossini et al. 2015).

The use of MRI neuronavigation is crucial for accurately locating cortical representations (Ruohonen and Karhu 2010). It has been shown that cortical representations generated with navigated TMS (nTMS) are highly correlated with motor maps obtained via direct cortical stimulation (Tarapore et al. 2012). Currently, motor cortex mapping with TMS is widely used for both clinical and research purposes (Rotenberg et al. 2014). Navigated TMS is an FDA-approved method of presurgical motor mapping (Krieg et al. 2017). Moreover, motor cortex mapping with TMS is used to assess motor cortex reorganization and plasticity in healthy subjects and patients who suffer from strokes (Lüdemann-Podubecká and Nowak 2016), brain tumors (Barz et al. 2018), cerebral palsy (Wittenberg 2009), amyotrophic lateral

Handling Editor: Giacomo Koch.

✉ Andrey Yu. Chernyavskiy
andrey.chernyavskiy@gmail.com

[1] Research Center of Neurology, Moscow, Russia 125367

[2] Valiev Institute of Physics and Technology of Russian Academy of Sciences, Moscow, Russia 117218

sclerosis (Chervyakov et al. 2015) and other diseases (Rotenberg et al. 2014).

One way of analyzing muscle representations is the direct visualization of their cortical topography. Additionally, TMS maps are commonly described by integral numerical characteristics. Some examples include the representation area, amplitude-weighted area, the coordinates of the center of gravity and of the point with the highest MEP amplitude (Wilson et al. 1993), and the mean MEP amplitude (Kraus and Gharabaghi 2016). Such measures are collectively called motor representation parameters in this paper. Although we focus on the area and weighted area, the general approach to estimating parameter accuracy can be applied to any characteristic defined as a function of all the MEP values and stimulus locations in a map.

A challenging problem in TMS mapping is estimating the location and size of the motor representation based on MEP values obtained at a finite number of stimulation points (Julkunen 2014; Pitkänen et al. 2017; Novikov et al. 2018). Most existing methods of solving this problem use the MEP amplitudes to classify all the cortical points in the mapped area into two classes: those that belong to the representation and those that do not. The accuracy of this classification depends on the algorithm and the density of the stimulus locations (Brasil-Neto et al. 1992; Classen et al. 1998). Unlike approaches such as the average point-area method (Julkunen 2014), Voronoi tessellation is applicable in the case of unevenly spaced stimulation points. The method has shown good repeatability of the motor representation area assessed by the intraclass correlation coefficient (Julkunen 2014).

The interpretation of motor maps obtained by nTMS is complicated by the significant variability in the amplitudes of MEPs. Thus, according to Mäki and Ilmoniemi (2010), for the stimulation of the same cortical point, one-third of the largest responses are on average 10 times higher than one-third of the lowest responses. This variability in the MEP amplitudes translates into variability in the estimated integral characteristics of motor representations (Van De Ruit et al. 2015). Weiss et al. (2013) reported that the repeated mapping of muscles in healthy subjects showed shifts in the center of gravity by an average of 7 mm and that three representations of the same muscle obtained in different sessions exhibited a spatial overlap of only 24% of their volume.

A possible approach to increasing the accuracy of estimating the parameters of motor representations consists in optimizing the TMS mapping protocol, i.e., the choices of the stimulus density, intensity, interstimulus interval and other aspects of the experiment (Brasil-Neto et al. 1992; Classen et al. 1998). Currently, there is no standard optimal mapping protocol that provides the highest accuracy, and a review of 20 studies of the TMS mapping in stroke described a variety of employed stimulation point configurations, numbers of stimuli per point, and TMS intensities (Lüdemann-Podubecká and Nowak 2016). A comparison of alternative protocols requires a measure of the accuracy of estimating the motor representation parameters under a given protocol. Finding such a measure is a nontrivial task because both the 'true values' of the parameters and the statistical distributions of their estimates for a given mapping protocol are not directly available from experiment (Pitkänen et al. 2017).

The accuracy of estimating motor representation parameters has been examined in a number of papers; however, most of the related works are focused on the reliability between sessions (Mortifee et al. 1994; Wolf et al. 2004; Malcolm et al. 2006; Forster et al. 2014; Kraus and Gharabaghi 2016). For example, in (Julkunen 2014), different methods of estimating the motor representation areas, including the Voronoi tessellation method, are compared in terms of the intraclass correlation coefficient (ICC) measuring the proportion of the total variance attributable to the differences between subjects. Since the aim in TMS mapping is to obtain the most accurate picture of the corticospinal excitability at the time of the procedure, it can be argued that the most relevant quality characteristic is the within-session accuracy (rather than the between-session variability affected by both this accuracy and the consistent physiological fluctuations). Thus, unlike the majority of studies, in the present paper, we develop a method of assessing the within-session accuracy. The method is based on statistical bootstrapping (Efron 1979). To obtain the distributions of parameter estimates, we simulate the possible TMS mapping results by subsampling stimulus locations and the corresponding MEPs from maps with sufficient numbers of stimuli. This approach allows the assessment of both the variability and the bias of the estimates with respect to the values computed from the initial maps. The method is applied to a set of TMS maps processed using Voronoi diagrams. We find the dependency of the errors in the area and weighted area on the number of stimuli in the maps generated by bootstrapping. This information can be used to select an appropriate number of stimuli in studies that apply TMS mapping to particular problems. This number depends on the expected effect size since detecting a small effect is harder than detecting a large one. Thus, a small effect requires high accuracy, which in turn makes it necessary to apply a large number of stimuli (determined using the obtained dependencies).

As mentioned above, only a few papers have considered the within-session accuracy despite its importance for the selection of a reliable mapping protocol. Van De Ruit et al. (2015) used subsamples of stimulus locations and the corresponding MEPs to assess the within-session accuracy of the motor area estimation obtained by the pseudorandom walk mapping protocol and the surface approximation method. The authors used a single random sample for each

subject and every considered value of the number of stimuli, calculating the minimum number sufficient for reliability in terms of an ad hoc threshold on the correlation coefficient with the full map. However, due to the varying accuracy requirements in different research problems, it is important to consider a range of possible error thresholds, which can be done using the dependencies of the error values on the number of stimuli obtained in the present paper. Moreover, the statistical bootstrapping approach provides detailed information about the variability and bias of the estimates, unlike the single subsample method. Another paper where single subsamples were used is (Classen et al. 1998). In this study, the authors assessed the within-session accuracy of a grid-based mapping protocol for different numbers of stimulation sites and different numbers of stimuli per site. Notably, in the present work, we study a non-grid mapping protocol with the individual selection of the locations of the cortical points and the sequence of their stimulation for each subject.

In (Thickbroom et al. 1999), simulated TMS mapping data was generated in a different manner: at each stimulation point, MEPs were sampled from a normal distribution with the parameters estimated from the experiment. Although this paper is important as one of the first studies to simulate TMS maps, its methods have serious limitations: the normal approximation of the MEP amplitude distribution [which is closer to the lognormal one (Goetz et al. 2014)] and the fixed stimulus positions. Brasil-Neto et al. (1992) mentioned the usage of common bootstrapping for the analysis of the accuracy of obtaining the positions with maximal MEPs. However, this pioneer work lacked details of the calculation method and its results.

We should emphasize that the approach developed in the present work can be applied to different motor representation parameters (e.g., the center of gravity) and other map processing methods, such as spline interpolation.

Materials and Methods

Experiments

Subjects

Fifteen healthy subjects (12 women; median age 26; age quartiles 23 and 28.5) with no contraindications to TMS participated in the experiment. The study was conducted according to the declaration of Helsinki and approved by the local ethics committee. All volunteers signed an informed consent form before entering the study.

MRI Protocol

All subjects underwent an MRI to obtain anatomical data. The procedure was performed on a Siemens MAGNETOM Verio 3-Tesla MR scanner (Germany) and employed a 3D T1 gradient echo sequence (T1_mpr_sag_p2_iso: TR 1900 ms, TE 2.47 ms, 1 mm2 isotropic voxel, and 176 sagittal slices completely covering the brain).

Motor Cortex Mapping Protocol

An nTMS system (NBS eXimia Nexstim, Finland) was used for muscle representation mapping. A figure-of-eight biphasic coil with a diameter of 50 mm was used to deliver stimuli with a 280 μs duration (data from the NBS eXimia Nexstim User Manual). The induced electric field was estimated by NBS eXimia Nexstim software individually for each subject at a depth of 20–25 mm from the surface of the skull (data from the NBS eXimia Nexstim User Manual). MEPs were recorded using skin pregelled disposable electrodes (Neurosoft, Russia) from the dominant extensor digitorum communis (EDC) and the flexor digitorum superficialis (FDS) muscles (these muscles were chosen for the analysis due to the planned work on a brain-computer interface employing the imagination of movements caused by contractions of the EDC and FDS muscles). The active electrode was mounted on the muscle, and the reference electrode was placed on the styloid process of the radius (for the EDC muscle) or the styloid process of the ulna (for the FDS muscle). Navigated TMS mapping was performed with a stimulation intensity equal to 110% of the individual motor threshold for each muscle. The value of the motor threshold was considered to be the minimum intensity of stimulation for which 5 out of 10 stimuli produced MEPs with amplitudes greater than or equal to 50 μV. The interstimulus interval was randomized between 2 and 2.3 s. During the mapping procedure, the induced electric field was kept approximately perpendicular to the central sulcus and directed anteriorly (Raffin et al. 2015). The locations and sequence of stimulation points were determined individually for each subject considering the responses obtained at previous points. The mapping progressed in a given direction until two points were obtained without inducing MEPs. Each point was stimulated once. Each analyzed cortical muscle representation contained at least 250 stimulation points (mean ± SD: 298 ± 41 points).

Data Analysis

Parameters of Cortical Muscle Representations and the Voronoi Diagram Method

We analyzed 30 TMS motor maps (for the EDC and FDS muscles in each subject), and the following parameters

characterizing the cortical representations were determined: the area and amplitude-weighted area.

We defined these parameters based on the Voronoi diagram method of processing the data obtained by TMS mapping. The Voronoi diagram splits the cortical surface into regions (cells), each containing only one stimulation point. This approach provides a straightforward method of computing the area of a motor representation (Julkunen 2014) as the sum of the areas of the Voronoi cells corresponding to positive MEPs: $S = \sum_{m_i \geq t} S_i$, where m_i represents the MEP amplitudes, S_i represents the areas of the corresponding Voronoi cells, and $t = 50$ μV is the MEP threshold. The area of a motor representation is based only on its geometry, and the weighted area accounts for each Voronoi cell in proportion to the corresponding MEP amplitude: $S_w = \sum_{m_i \geq t} m_i S_i$. This parameter is sometimes called the map volume (Kraus and Gharabaghi 2016). A more detailed description of the Voronoi diagram method is presented in Appendix A.

The Voronoi diagram method was chosen because of its applicability in the case of a nonuniform stimulus density and minimal dependence on theoretical assumptions. Although the area computed by Julkunen (2014) using spline interpolation exhibited higher intraclass correlation coefficients than the area calculated using Voronoi tessellation in 3 out of 4 muscle representations considered, the ICC values were close (and were all greater than 0.8); thus, both of these methods are suitable for motor mapping.

Notably, the proposed bootstrapping-based approach to analyzing within-session variability is not limited to Voronoi diagrams and can be applied in conjunction with different methods of motor map processing, such as spline interpolation or convex hull methods. Moreover, motor map characteristics other than the area and weighted area (such as the coordinates of the center of gravity) can also be investigated using the same methodology. These applications of the present approach will be explored in future studies.

Statistical Bootstrapping as a Method of Assessing the Accuracy of the Parameters of Muscle Representations

The accuracy of area estimation increases with the stimulus density. The latter, however, is limited by the practical constraints on the feasible mapping time, and thus, it is of interest to study a range of possible densities. The area estimates exhibit variability due to two factors: variations in the positions of the stimuli and the variability of MEPs at a single cortical location.

Figure 1 demonstrates the variability in the representations and their parameters. Random selection of 100 stimuli (the middle and right maps) from a full map containing 424 stimuli (the left map) produced maps with different values of the area and weighted area. Moreover, a difference in shape can be observed between the full and reduced maps.

Thus, we need to characterize the accuracy of the representation area estimates obtained using reasonable numbers of stimuli applied during the mapping procedure. The area of a motor representation obtained from the Voronoi tessellation method depends on all the measured MEPs and stimulus locations, and an analytic description of the corresponding probability distribution is difficult to obtain. To address this problem, we developed a method based on statistical bootstrapping (Efron 1979), i.e., drawing random subsamples from a given sample to estimate the distribution of a certain statistic.

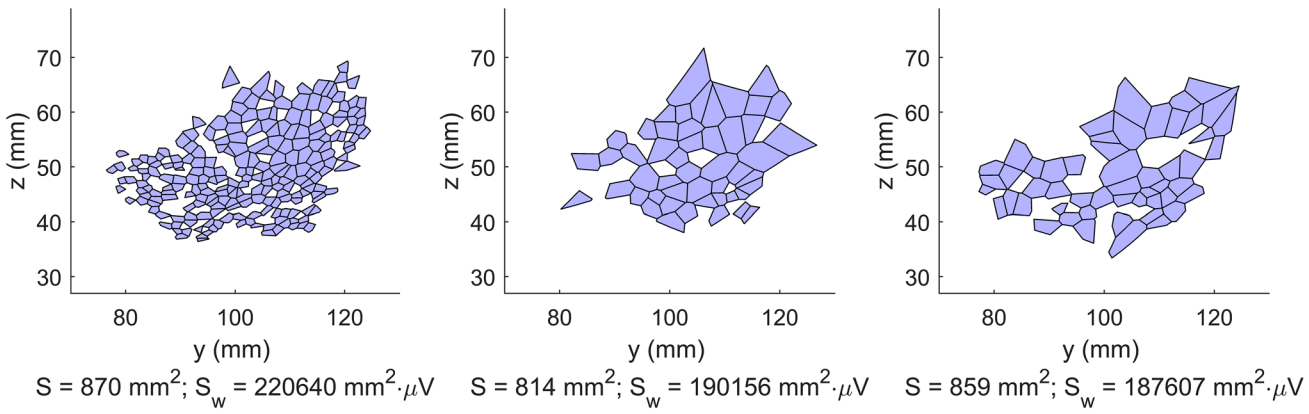

Fig. 1 Example of the influence of the number of stimuli and their positions on the shape, area and weighted area of a muscle (FDS) representation obtained using Voronoi tessellation. Left: full map (424 stimuli). Middle and right: maps obtained by randomly selecting 100 stimuli from the full map

In the present study, we applied this approach to the set of MEPs obtained in a given session of nTMS mapping by randomly choosing subsets of stimuli and computing the representation characteristics for these reduced maps. Considering one map and fixing the number of randomly selected stimuli, we can obtain a sample containing an arbitrary number of reduced maps. Every reduced map has a unique set of integral parameters, and for every parameter, we obtain a statistical distribution. Figure 2 shows example histograms of the area and weighted area for the map in Fig. 1 (5000 reduced maps, each with 100 stimuli, were generated). Such distributions can be used to analyze the accuracy of the estimates of the integral parameters obtained from maps with a given number of stimuli.

A short introduction to statistical bootstrapping is given in Appendix B.

Characteristics of the Accuracy of Muscle Representation Parameters

The specific values of motor representation parameters computed from experimental data can be viewed as estimators of the corresponding "actual" values (which would be obtained from a map with a very large number of stimuli). The accuracy of statistical estimators is characterized by two main properties: the bias, i.e., the systematic error, and the variability, i.e., the random error. Whereas the variability of motor representation parameters is commonly discussed in the literature, e.g. (Forster et al. 2014; Kraus and Gharabaghi 2016), the possible existence of a finite-sample bias has received less attention. It is important to characterize the bias because it can produce spurious effects and complicate comparing the results obtained using different mapping protocols.

Normalized Standard Deviation

The variability in representation parameters between bootstrap-generated maps can be characterized by the standard deviation (SD), denoted $SD(V_b)$, where V_b is the bootstrapped parameter. However, when pooling data from different subjects, we must remember that the SD can depend on the actual value of the parameter (denoted V). If we assume that large maps can approximately be thought of as scaled versions of small maps, the SD of the area estimate of a representation will be proportional to the actual area, which we estimate by the area of the full map. Thus, the ratio $v = SD(V_b)/V$, termed the normalized standard deviation (nSD), will belong to the same distribution for all subjects and will characterize the relative within-subject variability of area estimates. We analyze the individual values of nSD, as well as the group mean and SD of this variability characteristic, as functions of the number of stimuli in the reduced maps.

Normalized Bias

It is important that the accuracy of an estimator is determined not only by the variance but also by the bias, i.e., the difference between the estimator's mean and the true value of the estimated parameter. For the same reasons as those discussed for the SD, we use the normalized bias $b = (E(V_b) - V)/V$, where V is the value of a parameter in the full map, V_b is the bootstrapped parameter, and E is the expectation.

Total Accuracy (Normalized RMSD)

The total accuracy of an estimator is characterized by its root-mean-square deviation (RMSD), which can be expressed as the square root of the sum of the estimator's squared bias and squared SD. After dividing by the actual value of the parameter, we can compute the normalized RMSD (nRMSD) as $\sqrt{b^2 + v^2}$ for each map, where b and v are the normalized bias and nSD, respectively. The group mean values, SDs, and 90th percentiles of this value were computed and analyzed.

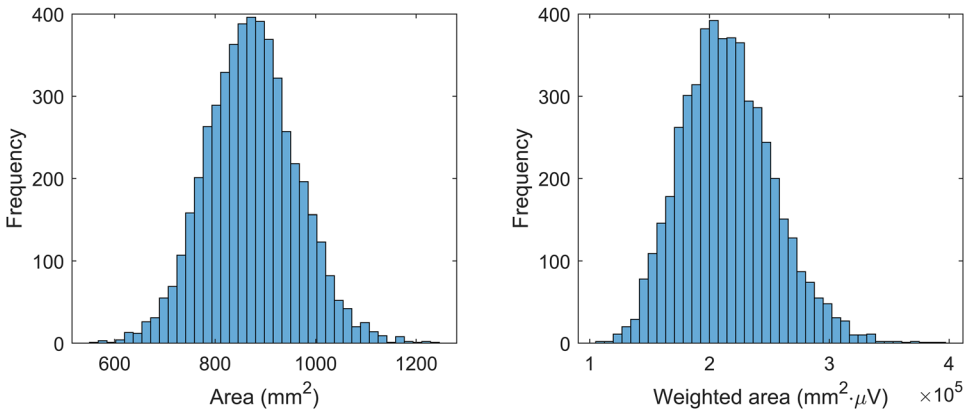

Fig. 2 Example of the distributions of the area and weighted area obtained for a sample of 5000 maps, each generated by randomly selecting 100 stimuli from the same full map as in Fig. 1 (424 stimuli)

Comparison of the Results for the FDS and EDC Muscles

We hypothesized that the values of the accuracy characteristics are independent of the particular muscle (FDS and EDC), and, consequently, the results can be presented using the joint data. After the computations, this statement was verified using the Wilcoxon signed rank test for all the accuracy characteristics (the nSD, normalized bias and nRMSD) and both muscle representation parameters (the area and amplitude-weighted area).

All data processing was performed in MATLAB R2017a (MathWorks, USA). Information on the implementation of the developed method of analysis and the mapping data availability is presented in Appendix C.

Results

Comparison of the Results for the FDS and EDC Muscles

The Wilcoxon signed rank test showed no significant difference between the accuracies of the FDS and EDC muscle representation parameters. All the accuracy characteristics (the nSD, normalized bias and nRMSD) and representation parameters (the area and amplitude-weighted area) demonstrated $p > 0.05$ for all the analyzed numbers of stimuli in the reduced maps. Accordingly, all the following results and figures are presented for the whole data consisting of 15 FDS and 15 EDC muscle mappings. By the muscle we mean any one of the EDC or FDS muscles.

The obtained independence from the choice between FDS and EDC leads to the hypothesis that this property also applies to all muscles. However, future research is needed to verify this hypothesis.

Normalized Standard Deviation of the Area and Weighted Area

Figure 3 shows the nSD values of the area and weighted area of a muscle representation as functions of the number of stimuli in the reduced maps generated by bootstrapping. As expected, the accuracy increases with the number of stimuli. To achieve an average nSD of 10% for the area, we need approximately 70 stimuli and 110 stimuli for the same nSD of the weighted area (the numerical values of the accuracy characteristics are given in Tables 1 and 2; the absolute values of the area and weighted area are presented in Table 3 for reference). A likely reason for the lower accuracy of the weighted area is the additional variability associated with the MEP amplitudes.

Figure 4 shows some individual examples of the dependence of the accuracy on the number of stimuli. An analysis of Figs. 3 and 4 suggests that it is reasonable to apply no less than 100–150 stimuli due to the steep decrease in the nSD in the left parts of the curves.

Table 1 Accuracy of the area estimation

N. stim.	nSD (mean)	nSD (SD)	N. bias (mean)	N. bias (SD)	Total (mean)	Total (SD)	Total (90th percentile)
50	0.134	0.022	− 0.018	0.025	0.138	0.022	0.170
60	0.118	0.021	− 0.004	0.021	0.120	0.021	0.155
70	0.103	0.019	0.003	0.018	0.105	0.019	0.135
80	0.092	0.018	0.007	0.015	0.093	0.018	0.122
90	0.083	0.016	0.010	0.013	0.085	0.016	0.111
100	0.075	0.015	0.010	0.012	0.077	0.015	0.100
110	0.069	0.013	0.010	0.012	0.070	0.014	0.090
120	0.063	0.013	0.011	0.012	0.065	0.013	0.085
130	0.058	0.012	0.010	0.011	0.060	0.013	0.077
140	0.054	0.012	0.010	0.010	0.055	0.012	0.075
150	0.050	0.011	0.008	0.010	0.051	0.012	0.067
160	0.045	0.010	0.008	0.008	0.047	0.010	0.061
170	0.042	0.010	0.007	0.008	0.043	0.010	0.057
180	0.039	0.009	0.006	0.007	0.040	0.010	0.052

N. stim. number of stimuli in the reduced maps generated by bootstrapping. *nSD* normalized standard deviation. *N. bias* normalized bias. *Total* normalized total accuracy (root mean square deviation). *Total (90th percentile)* 90th percentile of the normalized total accuracy. The columns denoted as (mean) and (SD) contain the mean values and standard deviations of the accuracy characteristics among the 30 mappings (2 muscle representations in each of the 15 healthy subjects)

Table 2 Accuracy of the weighted area estimation (same notation as in Table 1)

N. stim.	nSD (mean)	nSD (SD)	N. bias (mean)	N. bias (SD)	Total (mean)	Total (SD)	Total (90th percentile)
50	0.193	0.043	− 0.012	0.034	0.196	0.045	0.260
60	0.170	0.040	− 0.003	0.028	0.172	0.041	0.234
70	0.153	0.036	0.001	0.027	0.155	0.037	0.208
80	0.137	0.033	0.001	0.024	0.139	0.033	0.185
90	0.125	0.032	0.003	0.021	0.127	0.032	0.168
100	0.115	0.028	0.002	0.021	0.117	0.028	0.156
110	0.106	0.026	0.002	0.020	0.108	0.026	0.140
120	0.098	0.024	0.002	0.018	0.100	0.025	0.132
130	0.091	0.024	0.003	0.017	0.093	0.024	0.122
140	0.085	0.022	0.002	0.016	0.087	0.022	0.114
150	0.079	0.020	0.001	0.014	0.080	0.020	0.106
160	0.073	0.019	0.001	0.013	0.074	0.019	0.094
170	0.069	0.018	0.001	0.012	0.070	0.018	0.089
180	0.064	0.017	0.000	0.011	0.065	0.017	0.083

Normalized Bias of Area Parameters

Figures 5 and 6 show the group mean and individual values of the normalized bias as functions of the number of stimuli. The mean bias values of the area and weighted area are very small. The individual curves are qualitatively similar, but the group variance is considerable for small numbers of stimuli, which leads to the same recommendation of using no less than 100–150 TMS pulses. Notably, the observed small mean bias values result from accurate processing of Voronoi cells at the border of the map (Appendix A).

Total Accuracy (Normalized RMSD) of Area Parameters

Figure 7 shows the total error (nRMSD) of the area and weighted area for the reduced maps obtained by bootstrapping. Comparing these results with those in Figs. 3 and 5, we can conclude that for both the area and weighted area, the main source of inaccuracy is the variance. Notably, the nRMSD values (Fig. 7) are close to those of nSD (Fig. 3) due to the small bias.

To select an appropriate number of stimuli, it is useful to analyze the percentiles of the total error. Figure 8 shows the dependence of the 90th percentile of the total error on the number of stimuli. The area has a smaller error than the weighted area, with values below 10 and 17%, respectively, when using 100 stimuli in the mapping procedure and below 7 and 11% for 150 stimuli (in 90% of the motor representations).

Table 3 The values of the area and weighted area of the EDC and FDS muscle representations for all subjects

Subject	Area (mm^2)		Weighted area ($\mu V\ mm^2 \times 10^3$)	
	EDC muscle	FDS muscle	EDC muscle	FDS muscle
1	687	1035	234	493
2	338	417	103	78
3	539	633	118	177
4	383	377	63	39
5	362	670	215	299
6	280	291	48	45
7	309	359	48	51
8	439	476	215	237
9	429	562	71	130
10	554	744	201	432
11	505	499	206	82
12	576	870	121	220
13	586	468	226	91
14	603	474	186	68
15	650	543	252	166
Mean	483	561	154	174
SD	129	201	74	140

Auxiliary Data

Figure 9 demonstrates examples of cortical representations of the EDC and FDS muscles obtained by Voronoi tessellation for two random participants, also it shows the positions of stimuli with the highest MEP amplitudes. Table 4

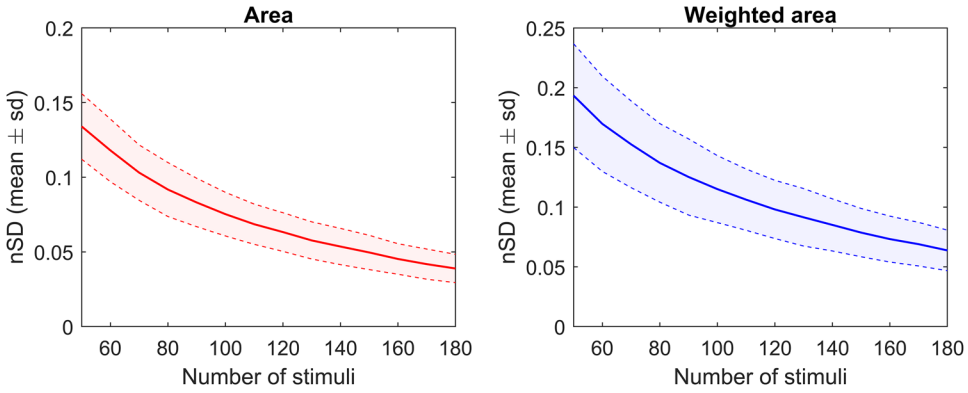

Fig. 3 Dependence of the variability (nSD) of the area and weighted area on the number of stimuli in the maps. The maps were generated by statistical bootstrapping from experimental data. The solid line represents the group mean and the dashed lines—the mean ± SD values. Smaller values correspond to more accurate estimates

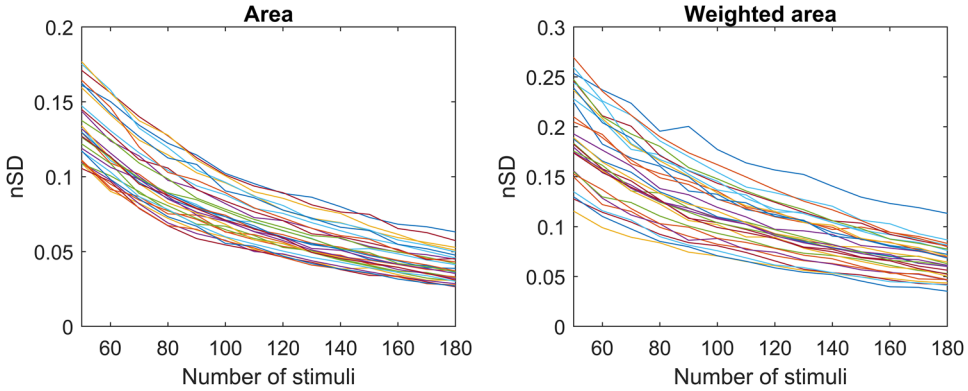

Fig. 4 Individual examples of the variability (nSD) of the area and weighted area as functions of the number of stimuli in the maps. The maps were generated by statistical bootstrapping from experimental data. Smaller values correspond to more accurate estimates

contains the values of the electric field (mean and SD values) and the stimulation intensities for all subjects.

Discussion

The main goal of the present study is to investigate the accuracy of estimating the area of cortical muscle representations using the Voronoi diagram method as a function of the number of TMS stimuli applied during the mapping procedure. The second goal is to use the obtained results to formulate methodological recommendations regarding the mapping protocol.

To evaluate the accuracy of the estimates of muscle representation parameters, we developed a new method based on statistical bootstrapping. The strength of the proposed approach is the possibility of simulating and exploring the distribution of the mapping results based on a single map with a sufficient number of stimuli. This objective is achieved by randomly selecting subsets of stimuli from the map and treating them as alternative mapping results. This approach can be applied to study any parameter that characterizes motor representations.

An important aspect of the proposed method is the focus on the accuracy associated with the mapping protocol and the data processing method rather than variations among subjects and sessions caused by other factors. Although changes between sessions have been investigated in a number of papers (Mortifee et al. 1994; Wolf et al. 2004; Malcolm et al. 2006; Forster et al. 2014; Kraus and Gharabaghi 2016), to our knowledge, this is one of the first studies to specifically address the influence of within-session fluctuations on the TMS mapping results.

Before discussing the results, we must emphasize that they were obtained only for healthy volunteers. The consideration of diseases may lead to different results due to changes in the geometry of muscle representations, e.g., their fragmentation into a number of separate patches.

Inaccuracies in the estimation of the area parameters are caused by two main factors: (1) variability related to

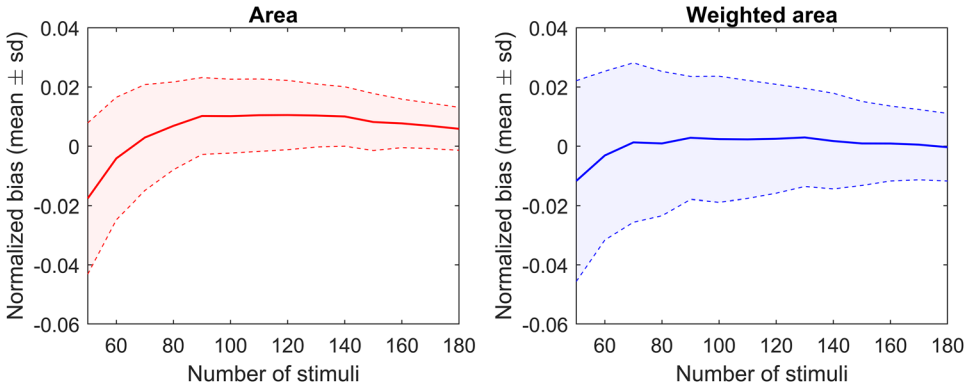

Fig. 5 Dependence of the normalized bias of the area and weighted area on the number of stimuli in the maps. The maps were generated by statistical bootstrapping from experimental data. The solid line represents the group mean and the dashed lines—the mean ± SD values. Smaller values correspond to more accurate estimates

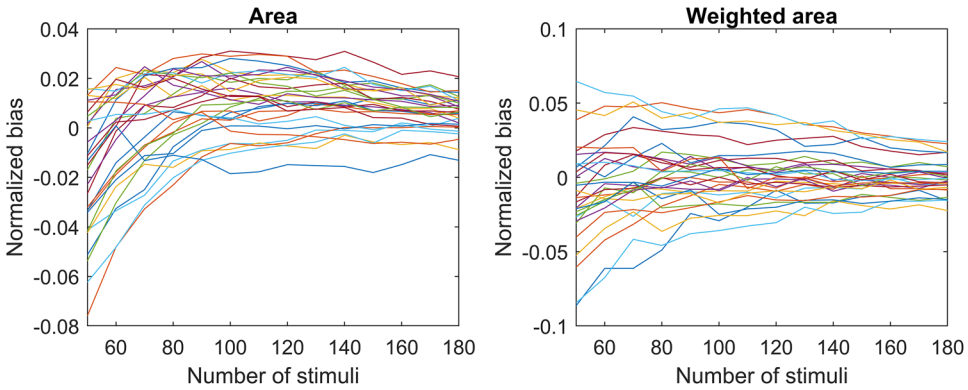

Fig. 6 Individual examples of the normalized bias of the area and weighted area as functions of the number of stimuli in the maps. The maps were generated by statistical bootstrapping from experimental data. Smaller values correspond to more accurate estimates

fluctuations in the positions of the stimuli and MEP values and (2) bias due to the finite number of stimuli. The analysis showed that the variability (measured by the nSD) was smaller for the area than for the weighted area, with little variation among subjects. Although the mean bias was small (Fig. 5), the individual values were considerable for many subjects (Fig. 6). Thus, comparing subject groups that have a systematic difference in the bias may lead to a spurious difference in the area values. Importantly, obtaining small mean bias values required accurate processing of the border cells of the Voronoi diagram (Appendix A). Estimators with a substantial bias are not uncommon in TMS mapping (Jonker et al. 2018), and this property must be considered in the data analysis.

The total error (nRMSD, Fig. 7) accounts for both sources of inaccuracy. Due to the small mean bias, the main source of inaccuracy is the variance. All error measures exhibited a steep decrease in the left parts of the curves (for small numbers of stimuli), which suggests the use of a protocol with no less than approximately 100 stimuli. The 90th percentiles of the total errors were below 7% for the area and 11% for the weighted area when using 150 stimuli (Fig. 8), which can thus be suggested as a reasonable value for achieving acceptable accuracy.

Similar to previous reports (Van De Ruit et al. 2015), the area displayed, on average, lower errors than the weighted area. It should be stressed that the two parameters characterize different aspects of motor representations: the size of the representation in the case of the area and the size and average MEP amplitude in the case of the weighted area. Consequently, the choice of the most useful parameter in a given study will depend on the population and the scientific question. For example, Bakulin et al. (2018) found that the weighted area was significantly lower in patients with local lower motor neuron syndrome compared to healthy subjects, but there was no significant difference in the area.

This study has several limitations. The developed bootstrapping-based approach requires maps with a number of stimuli significantly greater than that for which the parameter accuracy is to be assessed. While the present approach is universal, the specific accuracy estimates obtained in this paper are applicable to healthy subjects and the Voronoi tessellation processing method. Extensions to other situations will generally require additional studies. Moreover, these estimates were calculated only for the dominant EDC and FDS muscles. The analysis showed that the accuracy values for these two muscles have no significant difference. This leads to the hypothesis that the accuracy is independent from the choice of a particular muscle, however, this hypothesis must be verified.

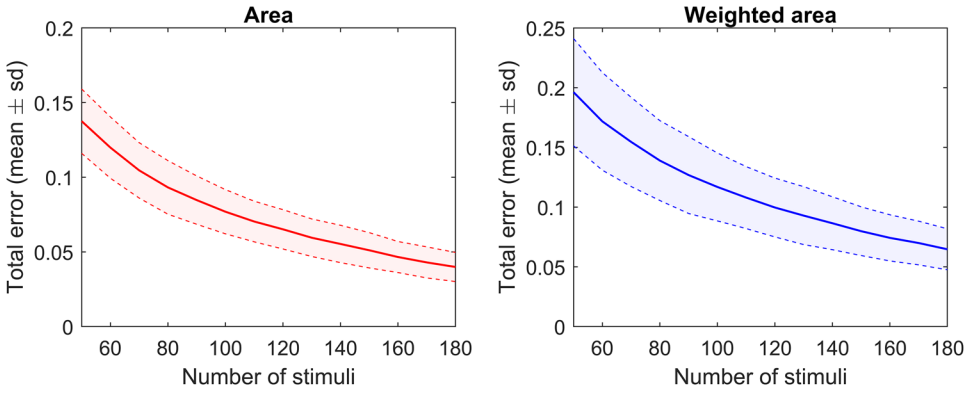

Fig. 7 The normalized total errors (nRMSD) in the estimates of the area and weighted area as functions of the number of stimuli in the maps. The maps were generated by statistical bootstrapping from experimental data. The solid line represents the group mean and the dashed lines—the mean ± SD values

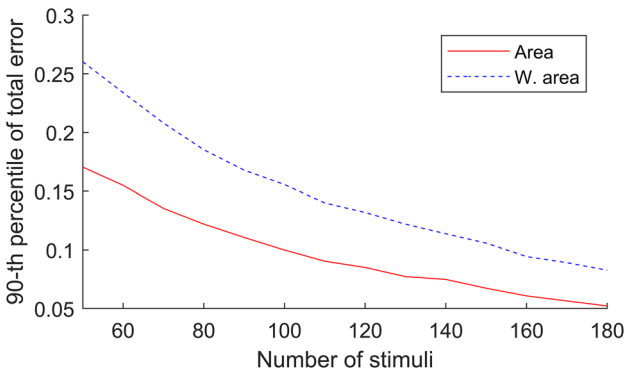

Fig. 8 The 90th percentiles of the total errors in the estimates of the area and weighted area as functions of the number of stimuli in the maps. The maps were generated by statistical bootstrapping from experimental data

Conclusions

The present study demonstrates that the TMS mapping of muscle representations coupled with the Voronoi diagram method of data processing can provide reasonable accuracy in estimating the area and weighted area of a representation. Specifically, we suggest using a mapping protocol with no less than 150 stimuli, which led to total relative errors of less than 7% for the area and 11% for the weighted area in 90% of the motor representations. These estimates can serve as approximate lower bounds for the magnitude of parameter differences between subject groups or conditions that can be detected with this mapping protocol. The obtained results can aid in planning future studies and in the clinical evaluation of cortical motor representations. Finally, the proposed bootstrapping-based method may be further applied to assess the accuracy of other integral parameters of TMS maps and evaluate and compare alternative mapping protocols.

Acknowledgements This study was supported by the Russian Science Foundation under Grant 17-75-10062.

Appendix A: Using the Voronoi Tessellation Method to Estimate the Area of Cortical Muscle Representations

Before the formal definition, it is useful to discuss the concept of the Voronoi diagram method by considering a common demonstrative example. Consider an area on the Earth with airports. Suppose an airplane must find the nearest airport. To do so, the pilots must determine the distances to all the airports and choose the shortest distance. However, this process can be optimized. Specifically, we can prepare a map in which all the locations with the same nearest airport are identically colored, and zones corresponding to different airports have different colors. Now, we can find a location on the map, look at its color, and instantly find the nearest airport. Such splitting of the plane is called a Voronoi diagram (or a Voronoi tessellation).

The method can be formally defined in the following way.

Consider a finite set Y of points y_i in a plane. The Voronoi diagram splits the plane as follows: each region V_i contains points for which the point y_i is the nearest among Y, or formally $x \in V_i \Rightarrow ||x - y_i|| = min_j ||x - y_j||$.

Spherical Voronoi Tessellation

In the present study, the Voronoi tessellation method was applied to stimulation points located on a cortical surface. The approximation of this surface by a plane limits the corresponding accuracy and can lead to the considerable distortion of the Voronoi cell areas at the periphery of the muscle representation. Thus, we used a more accurate approximation by a sphere and employed a spherical modification of the Voronoi tessellation (Na et al. 2002).

Processing of the Boundary Voronoi Cells

The planar Voronoi diagram splits the entire plane into a finite number of cells, so the outer cells have an infinite area. In the

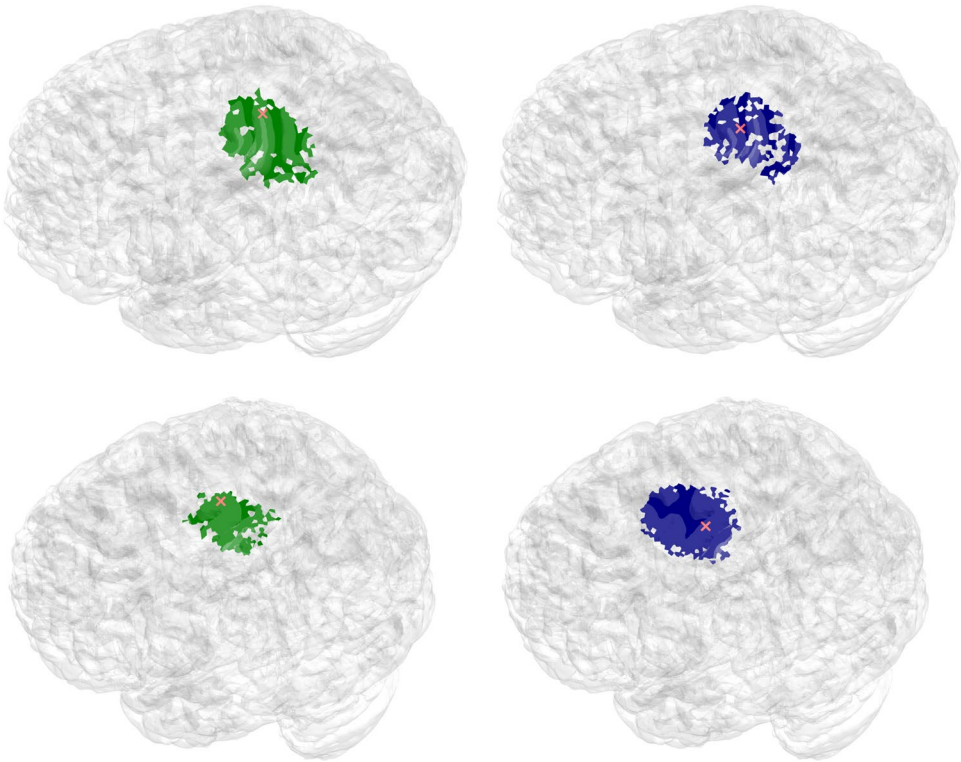

Fig. 9 An example of cortical representations of the EDC (left column) and FDS (right column) muscles obtained by Voronoi tessellation for two random participants. The crosses show the stimulation points with the maximal MEP amplitudes

Table 4 The values of the electric field (mean and SD values) and the stimulation intensities (per cent of maximum stimulator output) for all subjects

Subject	EDC muscle			FDS muscle		
	E-field mean (V/m)	E-field SD (V/m)	Intensity (%)	E-field mean (V/m)	E-field SD (V/m)	Intensity (%)
1	38.11	1.93	29	41.11	2.75	32
2	47.62	2.66	39	54.71	2.81	42
3	58.14	2.98	46	59.79	1.83	49
4	54.69	2.94	52	57.47	2.72	55
5	33.42	1.87	31	37.04	1.91	33
6	54.34	2.05	41	53.62	1.60	40
7	43.16	1.46	37	42.89	1.72	36
8	80.53	4.78	40	45.04	1.81	39
9	60.31	3.23	58	64.36	3.41	55
10	64.06	10.24	37	54.81	3.01	38
11	38.95	1.78	35	41.57	1.46	36
12	48.71	3.07	38	48.85	2.92	39
13	37.34	1.72	35	38.41	1.28	36
14	45.28	4.49	33	50.07	4.36	34
15	47.43	2.67	38	47.86	2.43	39
Mean	50.13	3.19	39.26	49.17	2.40	40.20
SD	12.31	2.17	7.67	8.19	0.84	7.26

case of the spherical approach and TMS mapping, we defined the corresponding cells as those that intersect the half of the sphere opposite the muscle representation position. In most cases, such cells correspond to stimuli with MEPs below the threshold. In our computational algorithm, we do not count such cells, including those with positive responses (this is a

rare situation). In addition to "infinite" cells, enormously large cells with positive MEPs can appear at the periphery if the border is poorly outlined (it is common to obtain 2–3 such cells in a reduced map generated by bootstrapping). Including the full areas of large border cells leads to a positive area bias, and removing these cells from computations leads to a negative bias. To avoid this problem, we identified cells with areas larger than $Q3 + 2(Q3 - Q1)$, where $Q1$ is the first and $Q3$ is the third quartile of all the areas of the "finite" Voronoi cells with positive MEPs and took $Q3$ as the areas of these cells in further computations of the parameters.

Appendix B: Introduction to Statistical Bootstrapping

A simple example can be given to illustrate to the bootstrapping method. Consider a coin (potentially an unfair one) flipped ten times, with a result of three heads (one point for each) and seven tails (zero points for each). Now, we have a statistical sample of ten results, and we can calculate some simple statistical characteristics, such as the average value (0.3) or standard deviation (0.483). However, if we must determine more complex characteristics, such as the probability of the average value of 93 tosses being higher than 0.54, a different approach is required. Statistical bootstrapping is a simple computational method for such tasks. For the sample of three heads and seven tails, let us randomly choose one of the results of the sample 93 times. By iterating this random choice of 93 results and comparing each average value with 0.54, we obtain a sample of positive/negative answers. Using this data, we can compute the desired probability. Therefore, the core concept of bootstrapping is the expansion of a statistical sample by Monte Carlo random sampling.

Although the presented example can be easily solved analytically, this may not be the case for more complex problems in which the use of bootstrapping is appropriate. In the present study, a method based on this approach was applied to evaluate the accuracy of the estimates of muscle representation parameters computed from TMS mapping data.

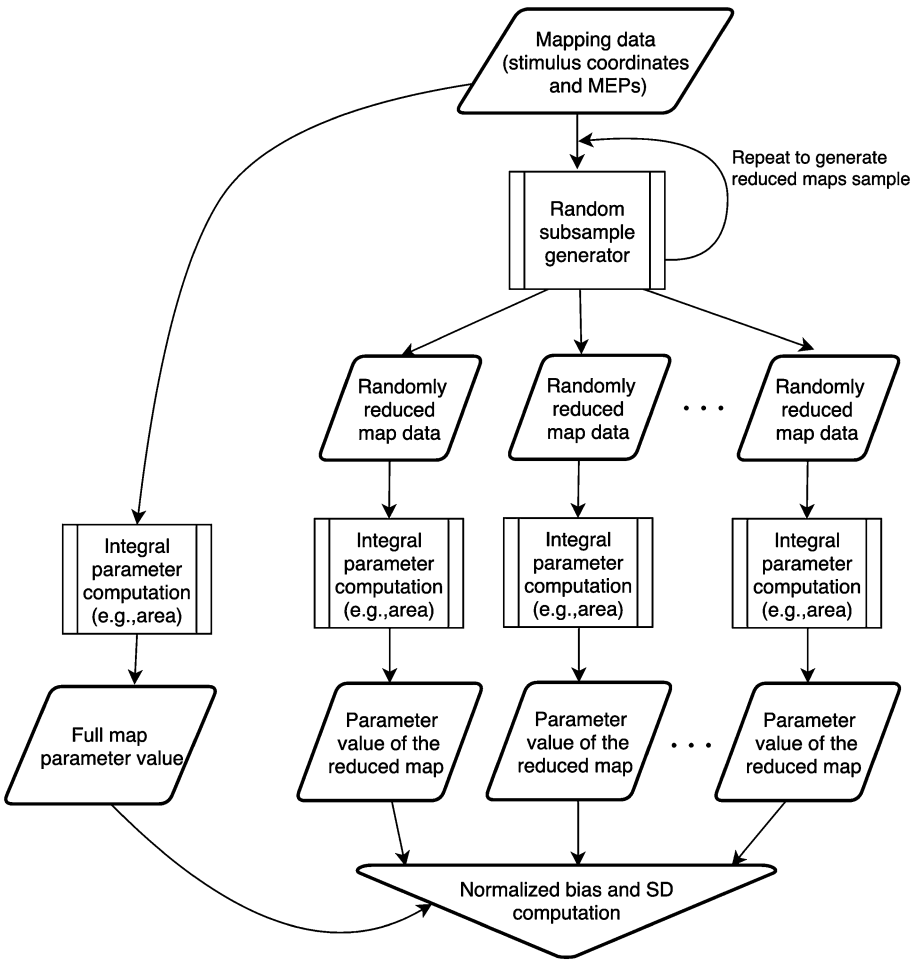

Fig. 10 The flow-chart diagram of the bootstrapping-based analysis of the data from a single TMS map

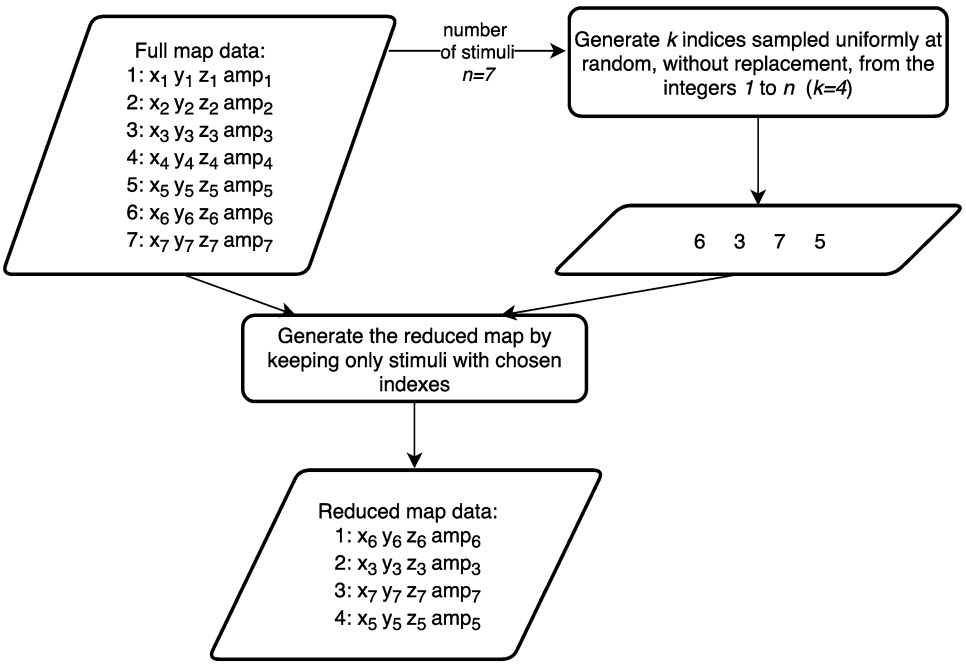

Fig. 11 The flow-chart diagram of the subroutine for the generation of a single reduced map

Appendix C: Implementation of the Bootstrapping-Based Analysis of the Accuracy of Cortical Representation Parameters Obtained Using TMS Mappings

Figure 10 contains the flow-chart diagram for the bootstrapping-based analysis of the data from a single TMS map. Figure 11 contains the flow-chart diagram of the subroutine for the generation of a single reduced map.

The Matlab implementation of the developed approach, the mapping data, and an example of the analysis of the accuracy for a sample cortical representation parameter (mean MEP amplitude multiplied by the maximal distance to the center of gravity) are available at the GitHub repository https://github.com/a-chernyavskiy/TMS-BS/. The computation of the parameters based on the Voronoi tessellation and other functions related to TMS mapping are planned to be added to the repository.

References

Bakulin IS, Poydasheva AG, Chernyavsky AY, Suponeva NA, Zakharova MN, Piradov MA (2018) Methods of detecting lesions of upper motor neuron in amyotrophic lateral sclerosis using transcranial magnetic stimulation. Ann Clin Exp Neurol 12:45–54

Barz A, Noack A, Baumgarten P, Seifert V, Forster M-T (2018) Motor cortex reorganization in patients with glioma assessed by repeated navigated transcranial magnetic stimulation-a longitudinal study. World Neurosurg 112:e442–e453. https://doi.org/10.1016/j.wneu.2018.01.059

Brasil-Neto JP, McShane LM, Fuhr P, Hallett M, Cohen LG (1992) Topographic mapping of the human motor cortex with magnetic stimulation: factors affecting accuracy and reproducibility. Electroencephalogr Clin Neurophysiol 85:9–16. https://doi.org/10.1016/0168-5597(92)90095-S

Chervyakov AV, Bakulin IS, Savitskaya NG, Arkhipov IV, Gavrilov AV, Zakharova MN, Piradov MA (2015) Navigated transcranial magnetic stimulation in amyotrophic lateral sclerosis. Muscle Nerve 51:125–131. https://doi.org/10.1002/mus.24345

Classen J, Knorr U, Werhahn KJ, Schlaug G, Kunesch E, Cohen LG, Seitz RJ, Benecke R (1998) Multimodal output mapping of human central motor representation on different spatial scales. J Physiol 512(Pt 1):163–179. https://doi.org/10.1111/J.1469-7793.1998.163BF.X

Di Lazzaro V, Ziemann U (2013) The contribution of transcranial magnetic stimulation in the functional evaluation of microcircuits in human motor cortex. Front Neural Circuits. https://doi.org/10.3389/fncir.2013.00018

Efron B (1979) Bootstrap methods: another look at the Jackknife. Ann Stat 7:1–26. https://doi.org/10.1214/aos/1176344552

Forster M-T, Limbart M, Seifert V, Senft C (2014) Test-retest reliability of navigated transcranial magnetic stimulation of the motor cortex. Oper Neurosurg 10:51–56. https://doi.org/10.1227/NEU.0000000000000075

Goetz SM, Luber B, Lisanby SH, Peterchev AV (2014) A novel model incorporating two variability sources for describing motor evoked potentials. Brain Stimul 7:541–552. https://doi.org/10.1016/j.brs.2014.03.002

Jonker ZD, Van Der Vliet R, Hauwert CM, Gaiser C, Joke HM, Van Der Geest JN, Donchin O, Ribbers GM, Frens MA, Selles RW (2018) TMS motor mapping: comparing the absolute reliability of digital reconstruction methods to the golden standard. Brain Stimul. https://doi.org/10.1016/j.brs.2018.11.005

Julkunen P (2014) Methods for estimating cortical motor representation size and location in navigated transcranial magnetic stimulation.

J Neurosci Methods 232:125–133. https://doi.org/10.1016/J.JNEUMETH.2014.05.020

Kraus D, Gharabaghi A (2016) Neuromuscular plasticity: disentangling stable and variable motor maps in the human sensorimotor cortex. Neural Plast. https://doi.org/10.1155/2016/7365609

Krieg SM, Lioumis P, Mäkelä JP, Wilenius J, Karhu J, Hannula H, Savolainen P, Lucas CW, Seidel K, Laakso A, Islam M, Vaalto S, Lehtinen H, Vitikainen A-M, Tarapore PE, Picht T (2017) Protocol for motor and language mapping by navigated TMS in patients and healthy volunteers; workshop report. Acta Neurochir (Wien). https://doi.org/10.1007/s00701-017-3187-z

Lüdemann-Podubecká J, Nowak DA (2016) Mapping cortical hand motor representation using TMS: a method to assess brain plasticity and a surrogate marker for recovery of function after stroke? Neurosci Biobehav Rev 69:239–251. https://doi.org/10.1016/j.neubiorev.2016.07.006

Mäki H, Ilmoniemi RJ (2010) EEG oscillations and magnetically evoked motor potentials reflect motor system excitability in overlapping neuronal populations. Clin Neurophysiol 121:492–501. https://doi.org/10.1016/j.clinph.2009.11.078

Malcolm MP, Triggs WJ, Light KE, Shechtman O, Khandekar G, Gonzalez Rothi LJ (2006) Reliability of motor cortex transcranial magnetic stimulation in four muscle representations. Clin Neurophysiol 117:1037–1046. https://doi.org/10.1016/J.CLINPH.2006.02.005

Mortifee P, Stewart H, Schulzer M, Eisen A (1994) Reliability of transcranial magnetic stimulation for mapping the human motor cortex. Electroencephalogr Clin Neurophysiol Potentials Sect 93:131–137. https://doi.org/10.1016/0168-5597(94)90076-0

Na H-S, Lee C-N, Cheong O (2002) Voronoi diagrams on the sphere. Comput Geom 23:183–194. https://doi.org/10.1016/S0925-7721(02)00077-9

Novikov PA, Nazarova MA, Nikulin VV (2018) TMSmap—software for quantitative analysis of TMS mapping results. Front Hum Neurosci 12:239. https://doi.org/10.3389/fnhum.2018.00239

Pitkänen M, Kallioniemi E, Julkunen P, Nazarova M, Nieminen JO, Ilmoniemi RJ (2017) Minimum-norm estimation of motor representations in navigated TMS mappings. Brain Topogr 30:711–722. https://doi.org/10.1007/s10548-017-0577-8

Raffin E, Pellegrino G, Di Lazzaro V, Thielscher A, Siebner HR (2015) Bringing transcranial mapping into shape: Sulcus-aligned mapping captures motor somatotopy in human primary motor hand area. Neuroimage 120:164–175. https://doi.org/10.1016/j.neuroimage.2015.07.024

Rossini PM, Burke D, Chen R, Cohen LG, Daskalakis Z, Di Iorio R, Di Lazzaro V, Ferreri F, Fitzgerald PB, George MS, Hallett M, Lefaucheur JP, Langguth B, Matsumoto H, Miniussi C, Nitsche MA, Pascual-Leone A, Paulus W, Rossi S, Rothwell JC, Siebner HR, Ugawa Y, Walsh V, Ziemann U (2015) Non-invasive electrical and magnetic stimulation of the brain, spinal cord, roots and peripheral nerves: basic principles and procedures for routine clinical and research application. An updated report from an I.F.C.N. Committee. Clin Neurophysiol 126:1071–1107. https://doi.org/10.1016/J.CLINPH.2015.02.001

Rotenberg A, Horvath JC, Pascual-Leone A (2014) Transcranial magnetic stimulation. Humana Press, New York

Ruohonen J, Karhu J (2010) Navigated transcranial magnetic stimulation. Neurophysiol Clin Neurophysiol 40:7–17. https://doi.org/10.1016/J.NEUCLI.2010.01.006

Tarapore PE, Tate MC, Findlay AM, Honma SM, Mizuiri D, Berger MS, Nagarajan SS (2012) Preoperative multimodal motor mapping: a comparison of magnetoencephalography imaging, navigated transcranial magnetic stimulation, and direct cortical stimulation. J Neurosurg 117:354–362. https://doi.org/10.3171/2012.5.JNS112124

Thickbroom GW, Byrnes ML, Mastaglia FL (1999) A model of the effect of MEP amplitude variation on the accuracy of TMS mapping. Clin Neurophysiol 110:941–943. https://doi.org/10.1016/S1388-2457(98)00080-7

Van De Ruit M, Perenboom MJL, Grey MJ (2015) TMS brain mapping in less than two minutes. Brain Stimul 8:231–239. https://doi.org/10.1016/j.brs.2014.10.020

Weiss C, Nettekoven C, Rehme AK, Neuschmelting V, Eisenbeis A, Goldbrunner R, Grefkes C (2013) Mapping the hand, foot and face representations in the primary motor cortex—retest reliability of neuronavigated TMS versus functional MRI. Neuroimage 66:531–542. https://doi.org/10.1016/j.neuroimage.2012.10.046

Wilson SA, Thickbroom GW, Mastaglia FL (1993) Transcranial magnetic stimulation mapping of the motor cortex in normal subjects. J Neurol Sci 118:134–144. https://doi.org/10.1016/0022-510X(93)90102-5

Wittenberg GF (2009) Motor mapping in cerebral palsy. Dev Med Child Neurol 51:134–139. https://doi.org/10.1111/j.1469-8749.2009.03426.x

Wolf SL, Butler AJ, Campana GI, Parris TA, Struys DM, Weinstein SR, Weiss P (2004) Intra-subject reliability of parameters contributing to maps generated by transcranial magnetic stimulation in able-bodied adults. Clin Neurophysiol 115:1740–1747. https://doi.org/10.1016/j.clinph.2004.02.027